ARTICLE NO. 79-0555R

Erosion Prediction near a Stagnation Point Resulting from Aerodynamically Entrained Solid Particles

J. A. Laitone*
Lawrence Berkeley Laboratory, University of California, Berkeley, Calif.

An analytic solution is obtained for the inviscid flow of a two-phase gas-solid mixture near a stagnation point. For this type of flow the momentum equilibration parameter, which is a measure of a particle's momentum, is found to be the unique determinant of particle trajectories. It is shown that values of this parameter less than one-fourth identify particles which never impact with a boundary. The closed-form solution is applied to an erosion model to predict the relative erosion distribution along the boundary. The erosion rate is found to be proportional to the particle velocity raised to the exponent of 4.0.

Nomenclature

E = relative erosion rate
J_∞ = particle number flux, freestream
M = particle mass flux
$N_{p\infty}$ = particle number density, freestream
q = particle impact speed
t = time
U = fluid velocity, freestream
v_p = particle velocity (u_p, v_p)
v = fluid velocity (u,v)
W = complex potential
X = characteristic length x direction ($x=X$ with $u=u_p=U$)
Y = characteristic length y direction ($y=Y$ with $v=v_p=V$)
Y_0 = particle impact coordinate
z = nondimensional time
z_s = nondimensional time when particle impacts
α = relative angle between particle path and wall surface
β = particle initial y/Y-coordinate
γ = scaling factor $\gamma = X/Y$
σ = particle radius
ρ = gas density
ρ_s = mass of particle per unit volume of particle material
τ = momentum equilibration time
λ = momentum equilibration length (nondimensional)
μ = gas viscosity
ν = gas kinematic viscosity

Introduction

FOR many years, gas-solid particle flows have interested scientists and engineers. Gas-particle flow phenomena are important in sedimentation pipe flows, fluidized beds, and transport processes. More recently the fields of propulsion, combustion, and energy conversion have stimulated new interest in this area of two-phase flow.

Presented as Paper 79-0555 at the AIAA 15th Annual Meeting and Technical Display, Washington, D.C., Feb. 6-8, 1979; submitted Feb. 13, 1979; revision received June 29, 1979.

Index categories: Multiphase Flows; Structural Durability, including Fatigue and Fracture.

*Research Assistant, Department of Mechanical Engineering. Student Member AIAA.

In particular, magnetohydrodynamic coal energy conversion, geothermal conversion, and coal gasification are three areas where a thorough understanding of gas-solid flows and the subsequent erosion is crucial.

This study treats the problem of determining the particle trajectories near a stagnation point. This is a critical area arising in a corner flow, flow into a flat plate, and flows over closed bodies such as cylinders and blades.

As a specific application, the gas-particle flow typical of a coal gasification system is analyzed. The particle impact speed, impact angle, and density distribution along the boundary are employed in a simple model of erosion prediction. In this way the primary aerodynamic factors that influence erosion are identified.

Two-Phase Model

The equations of motion of a particle in a steady stream with velocity components u,v have been derived[1] and are presented here in the following form:

$$\frac{Du_p}{Dt} = \frac{u-u_p}{\tau} \tag{1}$$

$$\frac{Dv_p}{Dt} = \frac{v-v_p}{\tau} \tag{2}$$

where

$$\tau = (2/9)(\rho_s \sigma^2/\mu)$$

It is assumed in this study that the dispersed particle phase is sufficiently dilute so that the mixture behaves as if it were made up of the continuous phase alone. Therefore, the particles do not significantly affect the continuous phase. Furthermore, the particle Reynolds number is assumed to be of order unity. Thus the volume force acting on the particle has the form of the Stokes' drag law.

These conditions arise in many two-phase flows. For instance, in the domain of the pressure vessel of a coal gasifier the gas velocity through the vessel is high enough so that the inviscid flow approximation is valid. However, the particle's (100-400 μ diam) slip velocity through the gas is small enough so that the Reynolds number based on particle diameter and slip velocity is less than unity. In this case the particles experience a highly viscous flow locally while the bulk gas flow can be treated as inviscid.

As a particle leaves the inviscid domain and passes into a boundary layer near a wall, these approximations fail; but, since the gas flow Reynolds number is large, the boundary layer is exceedingly thin. Since the distance traversed in the

boundary layer over which drag forces act is small, the work done on the particle by the gas is small. For particles approaching a wall at nearly normal impact angles, the boundary layer effects are negligibly small. It has been shown by Drew[2] that Eqs. (1) and (2) hold for inviscid gas flow when the flow Reynolds number is high, the particle volume fraction is of order 10^{-3}, and the particle momentum equilibration length parameter is of order unity.

Other assumptions are:

1) The particles are spherical and all of constant size.

2) Pressure, lift, gravitational, and viscous forces are negligible.

3) Brownian motion is negligible.

4) The continuous phase is incompressible.

Since $u_p = Dx/Dt$ and $v_p = Dy/Dt$, substitution into Eqs. (1) and (2) yields

$$\tau \frac{d^2x}{dt^2} + \frac{dx}{dt} - u = 0 \tag{3}$$

$$\tau \frac{d^2y}{dt^2} + \frac{dy}{dt} - v = 0 \tag{4}$$

Now consider the inviscid flow near the stagnation point. The complex potential is given outside the thin boundary layer as

$$W = -\tfrac{1}{2}\frac{U}{X}z^2$$

where X is some distance ahead of the stagnation point where free stream conditions exist ($u = -U$). The velocity components corresponding to this flow are

$$u = -\frac{U}{X}x \tag{5}$$

$$v = \frac{U}{X}y \tag{6}$$

To make a change of variables, let

$$z = t/\tau \text{ and } \lambda = \frac{\tau U}{X} = \frac{2}{9}\frac{\rho_s}{\rho}\frac{UX}{\nu}\frac{\sigma^2}{X^2}$$

where λ is the momentum equilibration length parameter. (λ is a similarity variable for this particular two-phase flow.) Physically, λ is a number that indicates the nondimensional distance required for a particle to travel in order to reduce its initial slip velocity by e^{-1}. Likewise, τ is referred to as the momentum equilibration time.

Equations (3) and (4) with (5) and (6) become

$$\frac{d^2x}{dz^2} + \frac{dx}{dz} + \lambda x = 0 \tag{7}$$

$$\frac{d^2y}{dz^2} + \frac{dy}{dz} - \lambda y = 0 \tag{8}$$

Solution Procedure

Equation (8) has solution

$$y = A_1 e^{r_1 z} + A_2 e^{r_2 z} \tag{9}$$

$$r_1 = -\tfrac{1}{2} + \tfrac{1}{2}(1+4\lambda)^{1/2} \qquad r_2 = -\tfrac{1}{2} - \tfrac{1}{2}(1+4\lambda)^{1/2} \tag{10}$$

Equation (7) has solutions of different form depending on the value of λ.

Case $\lambda < 1/4$

Here

$$x = A_3 e^{r_3 z} + A_4 e^{r_4 z} \tag{11}$$

$$r_3 = -\tfrac{1}{2} + \tfrac{1}{2}(1-4\lambda)^{1/2}, \qquad r_4 = -\tfrac{1}{2} - \tfrac{1}{2}(1+4\lambda)^{1/2} \tag{12}$$

To solve for A_3 and A_4, assume an initial condition that at the plane $x = X$ the particles have the gas stream velocity

$$u_p = -U = \frac{dx}{dt} = \frac{1}{\tau}\frac{dx}{dz} \tag{13}$$

Now if $t = 0$ ($z = 0$) when $x = X$, then from Eq. (11), $X = A_3 + A_4$, and Eq. (13) gives

$$(r_3 + \lambda)A_3 + (r_4 + \lambda)A_4 = 0$$

Thus

$$\frac{x}{X} = \left(\frac{r_4 + \lambda}{r_4 - r_3}\right)e^{r_3 z} + \left(\frac{r_3 + \lambda}{r_3 - r_4}\right)e^{r_4 z} \tag{14}$$

The particles that are at some initial position X traveling with the gas will hit the plate, provided that $X = 0$ for some finite z_s. Otherwise, the particles will only approach the plate asymptotically. Thus,

$$z_s = \frac{1}{r_3 - r_4}\ln\left(\frac{r_3 + \lambda}{r_4 + \lambda}\right)$$

Now $r_3 - r_4 = (1-4\lambda)^{1/2} > 0$ since $0 \le \lambda < 1/4$. The following equation is obtained by substituting for r_3 and r_4:

$$\frac{r_3 + \lambda}{r_4 + \lambda} = 1 + \frac{(1-4\lambda)^{1/2}}{\lambda - \tfrac{1}{2} - \tfrac{1}{2}(1-4\lambda)^{1/2}}$$

This shows that

$$\frac{r_3 + \lambda}{r_4 + \lambda} < 1$$

and therefore

$$z_s = \ln\frac{r_3 + \lambda}{r_4 + \lambda} < 0$$

Thus, $z_s < 0$ and at no time will the particles strike the plate.

Case $\lambda > 1/4$

Here

$$x = A_5 e^{-\frac{1}{2}z}\cos(\lambda - \tfrac{1}{4})^{1/2}z + A_6 e^{-\frac{1}{2}z}\sin(\lambda - \tfrac{1}{4})^{1/2}z \tag{15}$$

Assume an initial condition at $t = 0$ ($z = 0$) $x = X$ and

$$u_p = \frac{dx}{dt} = -U = \frac{1}{\tau}\frac{dx}{dz} \tag{16}$$

Then Eq. (15) gives $A_5 = X$

$$A_6 = \left(\frac{-\lambda + \tfrac{1}{2}}{(\lambda - \tfrac{1}{4})^{1/2}}\right)X$$

Thus

$$\frac{x}{X} = e^{-\frac{1}{2}z}\left[\cos(\lambda - \tfrac{1}{4})^{1/2}z + \frac{\tfrac{1}{2} - \lambda}{(\lambda - \tfrac{1}{4})^{1/2}}\sin(\lambda - \tfrac{1}{4})^{1/2}\right] \tag{17}$$

When $x=0$,

$$\tan(\lambda-1/4)^{1/2} z_s = \frac{(\lambda-1/4)^{1/2}}{(\lambda-1/2)} \tag{18}$$

As λ increases from 1/4 to 1/2, z_s decreases from π to $\pi/2$. As λ increases from 1/2 to ∞, z_s decreases from π to 0.

Thus, if $\lambda > 1/4$, the particles will always strike the plate, provided they are at some $x=X$ moving with the gas.

Case $\lambda = 1/4$

Here

$$x = A_7 e^{-1/2 z} + A_8 z e^{-1/2 z} \tag{19}$$

Assume an initial condition at $t=0$:

$$(z=0), x=X$$

and

$$u_p = \frac{dx}{dt} = -U = \frac{1}{\tau}\frac{dx}{dz}$$

Then Eq. (19) gives $A_7 = X$, $A_8 = 1/4 X$. Then,

$$\frac{x}{X} = e^{-1/2 z}(1 + 1/4 z) \tag{20}$$

The solution to Eq. (9) gives the y path.

Assume the initial condition $y=Y$ when $x=X$ at $z=0$. Then, from Eq. (9),

$$Y = A_1 + A_2 \tag{21}$$

For the second condition, we consider two cases.

Case A: $v_p = 0$

Then

$$0 = A_1 r_1 + A_2 r_2 \tag{22}$$

Thus

$$A_2 = Y r_1/(r_1 - r_2) \text{ and } A_1 = Y\left(\frac{-r_2}{r_1 - r_2}\right)$$

Thus

$$\frac{y}{Y} = (-r_2 e^{r_1 z} + r_1 e^{r_2 z})/r_1 - r_2 \tag{23}$$

See Fig. 1.

Case B: The Particles Follow the Streamline.

Initially

$$v_p = v = \frac{UY}{X} = \frac{dy}{dt} = \frac{1}{\tau}\frac{dy}{dz}$$

Combining this with Eq. (21), we obtain

$$A_1 = Y\frac{(\lambda - r_2)}{(r_1 - r_2)} \text{ and } A_2 = Y\left(1 - \frac{\lambda - r_2}{r_1 - r_2}\right)$$

The y trajectories are therefore given by

$$\frac{y}{Y} = \frac{\lambda - r_2}{r_1 - r_2} e^{r_1 z} + \frac{r_1 - \lambda}{r_1 - r_2} e^{r_2 z} \tag{24}$$

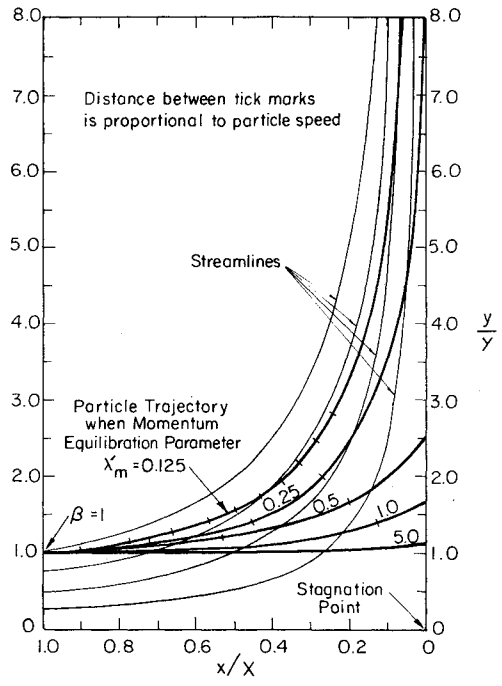

Fig. 1 Particle trajectories. The momentum equilibration parameter indicates the magnitude of a particle's momentum. When $\lambda > 10$, trajectories are almost entirely determined by initial conditions. For $\lambda \leq 0.25$, the particles are completely entrained in the gas flow and never impact with the wall.

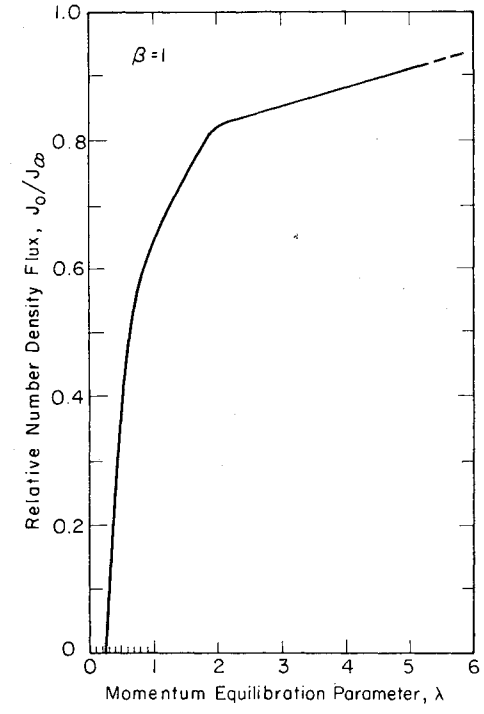

Fig. 2 Relative number density flux as a function of the momentum equilibration parameter. Particles with high momentum will impact with a number density approaching that found in the freestream region ($J_0/J_\infty \to 1$).

Method of Determining Impact Density, Speed, and Angle

As the momentum equilibration time τ increases (i.e., as λ increases), $z \to 0$. In the limit $\tau \to \infty$, if Y_0 is the y value for the particle striking the plane $x=0$, we find the following in case A, $Y_0/Y \to 1$; and in case B, $Y_0/Y \to 1$.

From Eqs. (23) and (24) we see that Y_0/Y is a function of λ only. Thus, the number density of particles along the wall ($x=0$) is constant for a given λ. Since all particles for which $y/Y<1$ will strike the plane at a distance less than Y_0, we arrive at the result

$$J_0 = \frac{Y}{Y_0} N_{p\infty} U = \frac{Y}{Y_0} J_\infty \tag{25}$$

if

$$N_{p\infty} = \frac{\text{number of particles in freestream}}{\text{unit volume}}$$

U = freestream gas velocity

$$J_0 = \frac{\text{number of particles striking wall}}{\text{unit area unit time}}$$

The variation of J_0/J_∞ with λ is shown in Fig. 2. For particles for which initially $y/Y=\beta$ ($0\le\beta\le 1$) and $\lambda > \frac{1}{4}$, the trajectories in case A are given by

$$\left.\frac{x}{X}\right|_{\beta=\beta} = e^{-\frac{1}{2}z}\left\{\cos(\lambda-\tfrac{1}{4})^{\frac{1}{2}}z + \left[\frac{\frac{1}{2}-\lambda}{(\lambda-\tfrac{1}{4})^{\frac{1}{2}}}\right]\sin(\lambda-\tfrac{1}{4})^{\frac{1}{2}}z\right\} = \left.\frac{x}{X}\right|_{\beta=1} \tag{26}$$

$$\left.\frac{y}{Y}\right|_{\beta=\beta} = \beta\{[\tfrac{1}{2}+\tfrac{1}{2}(1+4\lambda)^{\frac{1}{2}}]e^{[-\frac{1}{2}+\frac{1}{2}(1+4\lambda)^{\frac{1}{2}}]z} + [-\tfrac{1}{2}+\tfrac{1}{2}(1+4\lambda)^{\frac{1}{2}}]e^{[-\frac{1}{2}-\frac{1}{2}(1+4\lambda)^{\frac{1}{2}}]z}\}\Big/(1+4\lambda)^{\frac{1}{2}} = \beta\left.\frac{y}{Y}\right|_{\beta=1} \tag{27}$$

Furthermore, the speed on impact q (letting $\gamma=X/Y$) is given by (see Fig. 3)

$$\frac{q}{U} = \frac{1}{\lambda}\left[\left(\frac{1}{X}\frac{dx}{dz}\bigg|_{z=z_s}\right)^2 + \frac{\beta^2}{\gamma^2}\left(\frac{1}{Y}\frac{dy}{dz}\bigg|_{z=z_s}\right)^2\right]^{\frac{1}{2}} \tag{28}$$

where z_s is given in Eq. (18).

When $x=0$, $z=z_s$, and $y=Y_0$, and

$$\frac{1}{X}\frac{dx}{dz} = e^{-\frac{1}{2}z}\left\{\frac{-(\frac{1}{2})\lambda}{(\lambda-\frac{1}{4})^{\frac{1}{2}}}\sin(\lambda-\tfrac{1}{4})^{\frac{1}{2}}z - \lambda\cos(\lambda-\tfrac{1}{4})^{\frac{1}{2}}z\right\}$$

$$\frac{1}{Y}\frac{dy}{dz} = \frac{r_1 r_2}{r_1 - r_2}\{e^{r_2 z} - e^{r_1 z}\}$$

the angle of impact is

$$\alpha = \tan^{-1}\left(\frac{\gamma\frac{1}{X}\frac{dx}{dz}\Big|_{z=z_s}}{\beta\frac{1}{Y}\frac{dy}{dz}\Big|_{z=z_s}}\right) \tag{29}$$

By assigning successive values to β over the interval $0<y/Y\le 1$ and solving for a fixed λ, the particle trajectories, Eqs. (26) and (27), the impact speed, Eq. (28), and the impact angle (see Fig. 4), Eq. (29) are obtained for a distribution of similar particles. Since the particles are all of the same size and density, for a given distribution, no particle-particle collision will occur before impact with the wall. However, this model does not take into account particles that rebound from the wall.

The solution obtained in this section is general in nature and can be extended over a wide range of gas-particle flows as long as the constitutive assumptions are not invalidated. Having described the dynamic behavior of the solid particles entrained by the gas flow, it is possible to apply the results to a

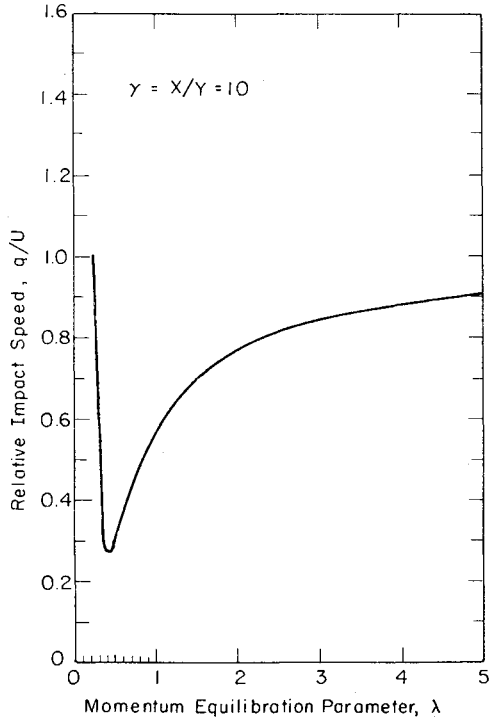

Fig. 3 Relative particle impact speed as a function of the momentum equilibration ration parameter. The increase in particle impact speed for $0.25<\lambda<0.40$ is due to the gas accelerating the particle away from the stagnation point.

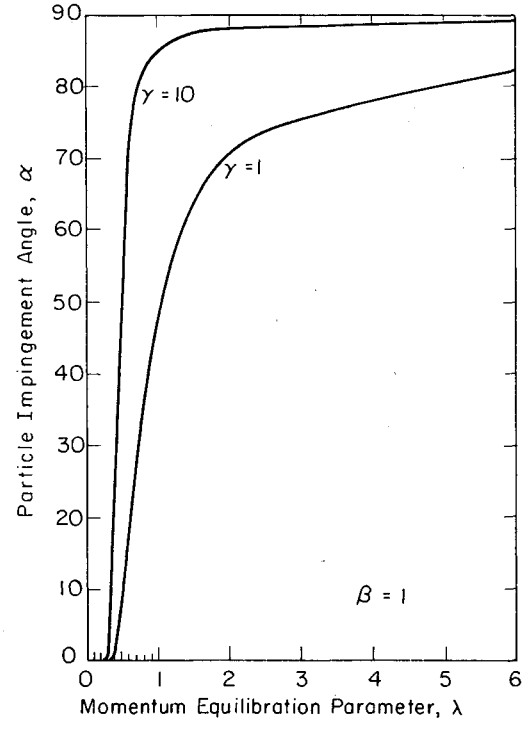

Fig. 4 Particle impingement angle as a function of momentum equilibration parameter. The initial position of a particle is given by $\gamma=X/Y$. Small values of γ correspond to thin bodies such as aerofoils.

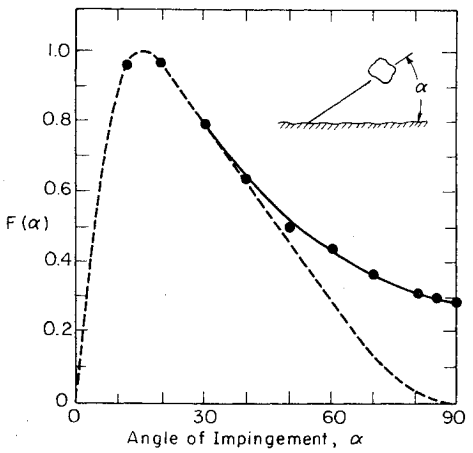

Fig. 5 General form of mass removal vs impingement angle for ductile erosion. Data points are for erosion of 1100-0 aluminum. Erosion curve was used to calculate relative erosion rate.

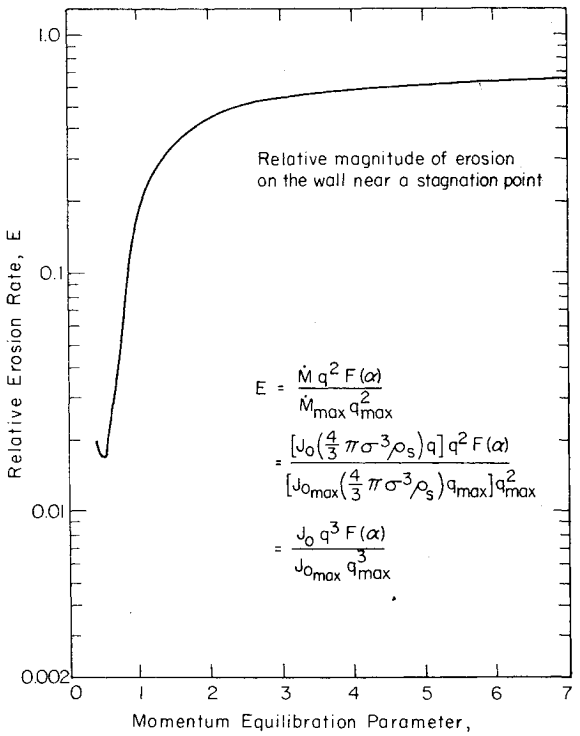

Fig. 6 Effect of momentum equilibration parameter on erosion. Since $E \sim q^3$, the curve exhibits characteristics predominated by the impact speed curve.

model for material erosion at a boundary. Erosion wear as measured on a weight-removal per weight of impacting particles is dependent on the velocity history of the impacting particles; since the solution form presented here gives an analytic expression for the absolute position of particles throughout the flow field, it is a simple matter to calculate how varying the flow conditions will change the erosion levels.

Application to Erosion Prediction on a Wall

As a specific example, consider the environment of a coal gasification system. Inside the pressure vessel, where erosion is most severe, the particles range from 100 to 400 μ in diam. The particle density is 0.96 g/cm^3, $\mu = 3.97 \times 10^{-4}$ g/cm-s, and $X = 91.44$ cm

A variety of erosion models can be applied to this system. An accurate model for ductile wall material has been developed by Finnie.[3] It assumes that the particles act as cutting tools, with the cutting depth a function of the hardness of the wall material.

The absolute magnitude of the erosion rate (volume of material removed per unit time) depends upon several physical parameters of the materials involved. However, the relative erosion rate can be found from knowing the impact speed, angle, and density using the following expression:

$$E = \frac{\dot{M} q^2 F(\alpha)}{\dot{M}_{\max} q^2{}_{\max}}$$

E = relative magnitude of erosion rate

$\dot{M}$ = mass flux of eroding particles

q = particle speed at impact

$F(\alpha)$ = scaling function (nondimensional) based on predicted and observed values of erosion of a ductile material by particles impinging at varying angles (see Fig. 5)

Rewriting, the relative erosion rate is:

$$E = \frac{J_0 4/3\pi\sigma^3\rho_s q) q^2 F(\alpha)}{(J_{0_{\max}} 4/3\pi\sigma^3\rho_s q_{\max}) q^2{}_{\max}} = \frac{J_0 q^3 F(\alpha)}{J_{0_{\max}} q^3{}_{\max}} \qquad (30)$$

The relative erosion is plotted in Fig. 6 as a function of the momentum equilibration parameter. The shape of the curve is clearly dictated by the impact speed variations since the erosion varies with the cube of the speed.

The intriguing shape of the erosion curve shown in Fig. 6 can be explained by examining the velocity components of the particles. As expected, particles with large λ are relatively unaffected by the continuous phase, and travel in straight lines with trajectories determined by the initial conditions. As λ decreases to a value of 2, the particles experience a very slight deceleration through the continuous phase in the x direction, along with an acceleration in the y direction due to the continuous phase accelerating away from the stagnation point. The overall increase in speed and erosion then is due to the magnitude of the vector sum of these two relatively large components.

Now for λ decreasing from 2 to 0.4, the particles experience a large deceleration in the x direction due to the increasing effect of the gas viscosity, leading to a small u velocity component and very low erosion levels.

This trend is suddenly reversed as λ decreases further toward 0.25. Here the particles are entrained in the continuous phase over a long time interval and, consequently, are accelerated with the continuous phase in the y direction. The impacts occur far from the stagnation point, with the large v velocity component dominating the impact speed and giving rise to the increased relative erosion rate. As noted previously, if $\lambda \leq 1/4$ the particles will not impact.

The minimum and maximum erosion points and respective values of the momentum equilibration parameter (namely, 0.4 and >2) determine the physical particle characteristics that are desirable (or detrimental) in an operating two-phase system, depending on whether erosion is to be minimized (wear reduction) or maximized (abrasion).

The effect of the initial particle velocity on the erosion rate is illustrated in Fig. 7. Intuitively, this is expected to be proportional to the square of the velocity; experiments with single particle impacts typically have exponent values between 2.2 and 2.8. However, the results show that the velocity exponent is normally greater than 2. Sheldon and Kanhere[4] predicted velocity exponents as high as 3. Grant and Tabakoff[5] found exponent values experimentally of the order of 4 in their work with uniform flow into a flat plate.

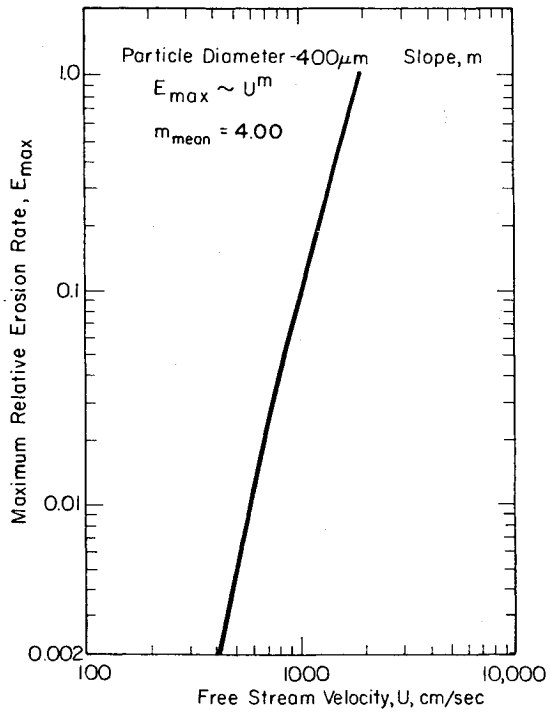

Fig. 7 Effect of freestream speed on erosion rate.

The mean exponent value found in Fig. 7 is 4.00, with the value attaining a maximum of 4.80 in the regime corresponding to λ equal to 1.0. This demonstrates the high velocity dependence when the particles are aerodynamically entrained.

Viscous effects near the wall should not influence these high exponent values of the velocity since they correspond to particles with large impact angles. Since the boundary layer is thin [i.e., $x/X = 0(10^{-3})$], only particles with very small impact angles will be slowed by the gas as it comes to rest at the wall.

Conclusions

An analytical model is developed to predict erosion occurring near a stagnation point flow. The model takes account of the aerodynamic drag on the particles, the impact angle, speed, and density, and determines the material removal along the wall. The solution is of a closed-form type and is based on analysis of a single particle.

The solution is readily applicable to a distribution of any number of like particles. However, when the number of particles becomes very large, the continuous phase is altered and the assumption of continuous phase variance under particle flows becomes invalid. Furthermore, if the flow Reynolds number or the momentum equilibration parameter is too small, the closed-form solution [Eqs. (25-30)] is invalidated. However, the usefulness of this solution is in its simplicity; the equations can be easily programmed on a hand calculator to provide a quick calculation of erosion levels for changing flow conditions and particle characteristics. Since the stagnation point area of turbine blades and other bodies experience the severest erosion in common industrial systems, this solution can be of aid in predicting erosion rates at the most critical wear point.

The momentum equilibration parameter is found to be a similarity parameter for this flow. A cutoff value of $\lambda \leq 0.25$ identifies those particles that never impact. The investigation shows that maximum erosion occurs for the value $\lambda \geq 2.0$. The erosion is found to be proportional to the velocity raised to the mean exponent of 4.00, which is confirmed by experiment.[5]

Acknowledgment

This work was supported by the Division of Materials Sciences, Office of Basic Energy Sciences, U.S. Department of Energy under Contract No. W-7405-ENG-48 through the Materials and Molecular Research Division of Lawrence Berkeley Laboratory.

References

[1] Taylor, G.I., "Notes on Possible Equipment and Technique for Experiments on Icing on Aircraft," *Aeronautical Research Committee Reports and Memoranda*, No. 2024, 1940, pp. 1-7.

[2] Drew, D.A., "Two-Phase Flows: Constitutive Equations for Lift and Brownian Motion and Some Basic Flows," *Archive for Rational Mechanics and Analysis*, Vol. 62, No. 2, 1976, pp. 149-163.

[3] Finnie, I., "Some Observations on the Erosion of Ductile Metals," *Wear*, Vol. 19, 1972, pp. 81-90.

[4] Sheldon, G.L. and Kanhere, A., "An Investigation of Impingement Erosion Using Single Particles," *Wear*, Vol. 21, 1972, pp. 195-209.

[5] Grant, G. and Tabakoff, W., "Erosion Prediction in Turbomachinery Resulting from Environmental Solid Particles," *Journal of Aircraft*, Vol. 12, May 1975, pp. 471-478.